

Article

The Role of Bulk Stiffening in Reducing the Critical Temperature of the Metal-to-Hydride Phase Transition and the Hydride Stability: The Case of $Zr(Mo_xFe_{1-x})_2-H_2$

Isaac Jacob ^{1,*}, Dotan Babai ^{2,†} , Matvey Bereznitsky ^{1,2} and Roni Z. Shneck ² ¹ Unit of Nuclear Engineering, Ben Gurion University of the Negev, Beer Sheva 84105, Israel; matveyb@bgu.ac.il² Department of Materials Engineering, Ben Gurion University of the Negev, Beer Sheva 84105, Israel; babaidot@gmail.com (D.B.); roni@bgu.ac.il (R.Z.S.)

* Correspondence: izi@bgu.ac.il

† Current address: Faculty of Engineering and Bar-Ilan Institute for Nanotechnology and Advanced Materials, Bar-Ilan University, Ramat-Gan 52900, Israel.

Abstract: This study aims to shed light on the unusual trend in the stabilities of $Zr(Mo_xFe_{1-x})_2$, $0 \leq x \leq 1$, hydrides. Both the rule of reversed stability and the crystal volume criterion correlate with the increased hydride stabilities from $x = 0$ to $x = 0.5$, but are in contrast with the destabilization of the end member $ZrMo_2$ hydride. The pressure-composition isotherms of $ZrMo_2-H_2$ exhibit very wide solid solubility regions, which may be associated with diminished H–H elastic interaction, u_{elas} . In order to discern this possibility, we measured the elastic moduli of $Zr(Mo_xFe_{1-x})_2$, $x = 0, 0.5, 1$. The shear modulus, G , shows a moderate variation in this composition range, while the bulk modulus, B , increases significantly and monotonically from 148.2 GPa in $ZrFe_2$ to 200.4 GPa in $ZrMo_2$. The H–H elastic interaction is proportional to B and therefore its increase cannot directly account for a decrease in u_{elas} . Therefore, we turn our attention to the volume of the hydrogen atom, v_H , which usually varies in a limited range. Two coexisting phases, a Laves cubic ($a = 7.826 \text{ \AA}$) and a tetragonal ($a = 5.603 \text{ \AA}$, $c = 8.081 \text{ \AA}$) hydride phase are identified in $ZrMo_2H_{3.5}$, obtained by cooling to liquid nitrogen temperature at about 50 atm. The volume of the hydrogen atom in these two hydrides is estimated to be $2.2 \text{ \AA}^3 / (\text{H atom})$. Some very low v_H values, have been reported by other investigators. The low v_H values, as well as the one derived in this work, significantly reduce u_{elas} for $ZrMo_2-H_2$, and thus reduce the corresponding critical temperature for the metal-to-hydride phase transition, and the heat of hydride formation. We suggest that the bulk stiffening in $ZrMo_2$ confines the corresponding hydride expansion and thus reduces the H–H elastic interaction.

Keywords: intermetallic hydrides; hydrogen atomic volume; $Zr(Mo_xFe_{1-x})_2$ pseudobinary intermetallics; critical temperature of metal to hydride phase transition; hydrogen–hydrogen elastic interaction; elastic moduli



Citation: Jacob, I.; Babai, D.; Bereznitsky, M.; Shneck, R.Z. The Role of Bulk Stiffening in Reducing the Critical Temperature of the Metal-to-Hydride Phase Transition and the Hydride Stability: The Case of $Zr(Mo_xFe_{1-x})_2-H_2$. *Inorganics* **2023**, *11*, 228. <https://doi.org/10.3390/inorganics11060228>

Academic Editor: Duncan H. Gregory

Received: 17 April 2023

Revised: 20 May 2023

Accepted: 23 May 2023

Published: 25 May 2023



Copyright: © 2023 by the authors. Licensee MDPI, Basel, Switzerland. This article is an open access article distributed under the terms and conditions of the Creative Commons Attribution (CC BY) license (<https://creativecommons.org/licenses/by/4.0/>).

1. Introduction

The present study demonstrates a significant impact of the bulk modulus on the hydride formation of the intermetallic compounds $ZrMo_2$ and TaV_2 . It would be instructive to consider at the outset some general factors determining the hydrogenation behavior of metal alloys. It is a well-known empirical rule that hydrogen-absorbing alloys or intermetallic compounds must contain at least one elementary metal forming a reversible hydride at nearly ambient conditions, e.g., Ref. [1]. The ability of the compounds to absorb hydrogen is thus determined by the metal–hydrogen interaction. In addition, the properties of the parent intermetallics provide some guidelines regarding the stability of the corresponding hydrides: (i) the rule of reversed stability—the more stable the original intermetallic, the less stable the resulting hydride [2]; (ii) the crystal volume criterion—the hydride stability increases with the increase in the original crystal volume [3]; (iii) the

crystal structure—sometimes alloys of identical or nearly identical chemical compositions crystallize in a completely different lattice structure. The one, presenting interstitial sites more abundant in hydride-forming elements, forms more stable hydrides. For example, the pseudobinary $U(Al_xNi_{1-x})_2$ system crystallizes in two different structures, a Laves phase structure in the compositional ranges $0 \leq x \leq 0.2$, $0.9 \leq x \leq 1$, and a ZrNiAl-type (Fe_2P -type) structure at $0.4 \leq x \leq 0.5$. The Laves phase compounds do not absorb hydrogen up to pressures of 100 atm, while the hydrides $UNiAlH_{2.5}$ and $UNi_{1.2}Al_{0.8}H_{2.35}$ are formed at that pressure range. This difference of hydrogen absorption is attributed to the presence of uranium-rich tetrahedral sites ($3U + 1(Ni,Al)$) in $U(Al_xNi_{1-x})_2$, $x = 0.4, 0.5$, as compared to the ($2U + 1(Ni,Al)$) sites in the Laves-phase compounds, where uranium is the hydride-forming element [4,5]; and (iv) we will consider in some detail the influence of the bulk elastic modulus on the critical temperature, T_c .

The metal to hydride phase transition in most hydrogen-absorbing intermetallic compounds is characterized by a critical temperature, T_c . A discontinuous transformation of the crystal lattice occurs below T_c , while above it the final hydride structure may be reached in a gradual, continuous way. This behavior imposes identical or very similar crystal structures of the original intermetallic compound and its corresponding hydride, besides the usual increase in the lattice volume upon hydrogenation. The metal to hydride phase transformation is driven by attractive hydrogen–hydrogen interaction, $-u$, which is composed of elastic and electronic parts [6].

$$u = u_{\text{elas}} + u_{\text{elec}}$$

The critical temperature, T_c , is related to the attractive H–H interaction:

$$T_c = u \times r/4k \quad (1)$$

r is the number of interstitial sites per metal atom available for hydrogen absorption and k is Boltzmann's constant ($1.38 \times 10^{-23} \text{ J K}^{-1}$). The corresponding units of u are J.

The form of the elastic part, u_{elas} , has been derived by several investigators, e.g., Refs. [6–8]:

$$u_{\text{elas}} = \left(1 - \frac{B}{B + \frac{4}{3}G}\right) B \frac{v_H^2}{V} \quad (2)$$

B and G are the bulk and shear moduli in Pa (N/m^2), respectively, v_H is the excess volume occupied by one hydrogen atom in the metal matrix in m^3 , and V is the average volume per metal atom in m^3 . u_{elas} is then obtained in J. u_{elas} is usually presented in eV by multiplying the value in J by the conversion factor $1 \text{ J} = 6.242 \times 10^{18} \text{ eV}$. The volume, v_H , of the hydrogen atom in the metal matrix and the term in the brackets usually do not change very much. Typical values of v_H stay in the range of $2.5\text{--}3 \text{ \AA}^3/\text{H atom}$, e.g., Ref. [6]. The bulk modulus, B , is then a leading term in u_{elas} . The physical reasoning for the increase in the long-range u_{elas} interaction with B is that larger B induces larger strain fields in the crystal lattice around a hydrogen atom and provides better linkage between the hydrogen atoms. The attractive elastic interaction is considered to play a main role in the metal-to-hydride phase transition. Fen Li et al. have proposed a repulsive screened Coulomb interaction between the hydrogen atoms in $TiCr_2H_x$ [9]. It was recently demonstrated that the electronic interaction may be repulsive, negligible, or attractive by considering the corresponding critical temperatures of the $ZrCr_2\text{-}H_2$ (<300 K), $ZrMn_2\text{-}H_2$ (564 K), and $Pd\text{-}H_2$ (565 K) systems in relation to their relevant elastic properties, Equations (1) and (2) [10].

This study aims at elucidating a puzzling behavior of the hydride stabilities in the $Zr(Mo_xFe_{1-x})_2$ system, as presented at MH2018 and subsequently published [11]. Figure 1 [11] exhibits pressure-composition isotherms, demonstrating increased monotonic stability of the $Zr(Mo_xFe_{1-x})_2$ hydrides for $x = 0, 0.2, 0.5$, but then this trend is reversed by a stability decrease for $x = 1$. Investigating these stability trends of the $Zr(Mo_xFe_{1-x})_2$ hydrides, in view of the guidelines listed above, requires a knowledge of relevant data, namely,

the heats of formation of the original intermetallic compounds, their crystal structures, lattice parameters, bulk and shear moduli, and the degree of expansion upon hydrogenation which determines v_H . Most of these data appear in the literature. In order to complete the required set, elastic properties have been determined in this work. In addition, we hydrogenated $ZrMo_2$ to the greatest possible extent under the available experimental conditions in our lab, attempting to settle some differing crystallographic results, associated with the volume of the hydrogen atom in $ZrMo_2$ hydride(s).

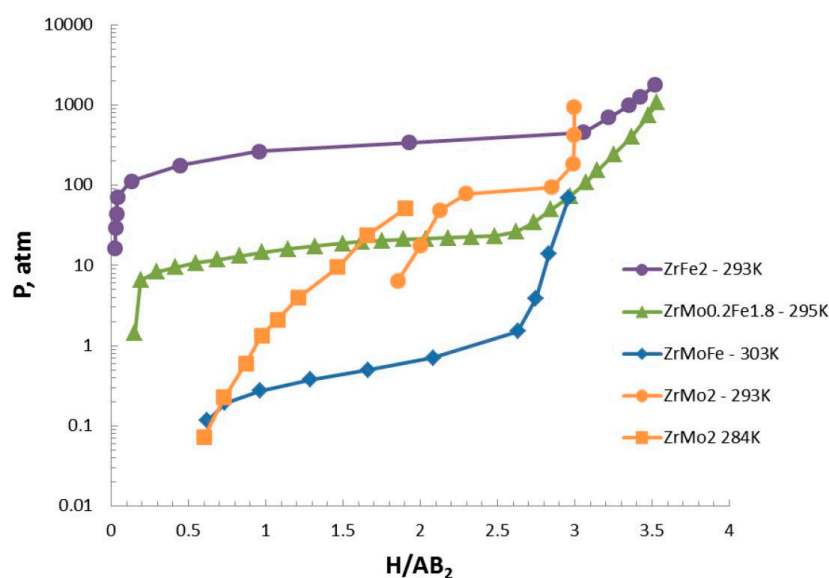


Figure 1. Pressure-composition isotherms of $Zr(Mo_xFe_{1-x})_2-H_2$ systems, $x = 0, 0.1, 0.5, 1$ at the indicated temperatures. (Reprinted with permission from Ref. [11] under license 5531441401625 by Elsevier).

2. Experimental Details

$Zr(Mo_xFe_{1-x})_2$, $x = 0, 0.5, 1$, samples were prepared by arc melting high-purity (~99.9%) elements on a water-cooled copper hearth. The pellets were homogenized by melting them at least three times, turning them over after each melting. The as-cast alloys were then sealed in argon-filled quartz ampules and annealed for 72 h at 1373 K. The crystal structure of the prepared compounds was determined and verified by X-ray diffraction (XRD) in a PW 1050/70 diffractometer from Philips, utilizing $Cu K_\alpha$ radiation of 1.5418 Å. Parallel-faced intermetallic slices of about 2.5 mm thickness were cut using a diamond sawing disk and subsequently polished to achieve a parallelism within the range of 3×10^{-6} m. The resulting parallel-faced samples were then subjected to sound velocity measurements using the pulse echo (PE) method. The frequency of the PE piezoelectric transducers for both the longitudinal and transverse modes was 5 MHz. The sound wave velocities were determined by measuring the time needed for the acoustic waves to travel forth and back between the opposite parallel faces of the sample. The densities of the samples were analyzed using the measured structural parameters. The obtained results were then compared to the measured Archimedes densities (both wet and dry) in order to determine the porosity ratio of the samples.

$ZrMo_2$ compound was hydrogenated at about 60 atm hydrogen pressure and room temperature in a home-built Sieverts system, equipped with 3.5, 60, and 100 atm pressure transducers. The amount of absorbed hydrogen in $ZrMo_2$ was calculated by considering the non-ideality of the hydrogen gas. For example, the difference between the real and the ideal hydrogen pressures at 100 atm and room temperature is about 6%. The reactor chamber, with the hydrogenated sample in it, was then very slowly cooled from room to liquid nitrogen temperature in order to enhance the hydrogen absorption. The equilibrium hydrogenation pressure decreases in an exponential way vs. the decreased temperature. Thus, decreasing the sample temperature at approximately constant pressure, as most

of the system is kept at ambient conditions, corresponds to significantly increasing the pressure at room temperature. Hydrogen absorption is expected to be practically none at very low temperatures, e.g., 78 K, because of extremely reduced kinetics. The very slow cooling is then intended to enable hydrogen absorption at intermediate temperatures, between 295 K and 78 K. Finally, a poisoning procedure was applied. (The purpose of the poisoning procedure is a contamination of the surface of the sample, for example by water vapor, without changing its bulk content. This contamination keeps the hydride intact and prevents its decomposition for long enough time in order to enable some experimental measurements at ambient conditions, e.g., XRD.) The hydrogen was evacuated from the reaction chamber, kept at liquid nitrogen temperature, and then the sample was exposed to the ambient atmosphere. The X-ray diffraction pattern of the air-exposed sample was immediately recorded without any additional precautions. The poisoning is considered successful provided two conditions are fulfilled: (i) the XRD pattern of the hydrogenated sample is significantly different from the pattern of the original compound; and (ii) the XRD pattern of the hydrogenated sample does not change or changes very slowly with time. These two conditions were satisfied in the present case of ZrMo_2 —see Section 3.1 below.

3. Results and Discussion

3.1. Structural and Elastic Properties of $\text{Zr}(\text{Mo}_x\text{Fe}_{1-x})_2$, $x = 0, 0.5, 1$

ZrFe_2 and $\text{Zr}(\text{Mo}_{0.5}\text{Fe}_{0.5})_2$ exhibited single Laves phases in their XRD patterns, while 95% Laves phase was obtained for ZrMo_2 (Figure 2). ZrFe_2 and ZrMo_2 crystallized in the cubic C15 phase with lattice constants 7.074 Å and 7.589 Å, respectively. These values are in fair agreement with the published data for ZrFe_2 (e.g., 7.074 Å [12]) and ZrMo_2 (e.g., 7.59 Å [13]). About 5% of Mo, with lattice constant $a = 3.185$ Å, was present along the ZrMo_2 pattern (Figure 2). The cubic crystal parameter of pure Mo is 3.147 Å [14]. The increased a value indicates the dissolution of some Zr into the molybdenum matrix. $\text{Zr}(\text{Mo}_{0.5}\text{Fe}_{0.5})_2$ presents a C14 hexagonal phase with lattice constants $a = 5.173$ Å and $c = 8.461$ Å, comparable to $a = 5.172$ Å and $c = 8.463$ Å [15] or $a = 5.130$ Å and $c = 8.440$ Å [16]. The longitudinal, v_L , and transverse, v_T , ultrasonic velocities, measured by the pulse-echo method, are presented in Table 1. They were used to calculate two elastic constants according to the relations $C_{11} = v_L^2\rho$ and $C_{44} = v_T^2\rho$, assumed to hold for polycrystalline isotropic samples (ρ is the sample density). Bulk, B , and shear, G , moduli were derived from the relations $B = C_{11} - 4C_{44}/3$ and $G = C_{44}$ (Table 1). Minor corrections of B and G were made in view of the small porosities of the samples [17,18]. The shear modulus changes moderately with the composition, x , along the $\text{Zr}(\text{Mo}_x\text{Fe}_{1-x})_2$ series, while the bulk modulus increases significantly and monotonically as a function of x . The variations of B and G are exhibited in Figure 3 and Table 1.

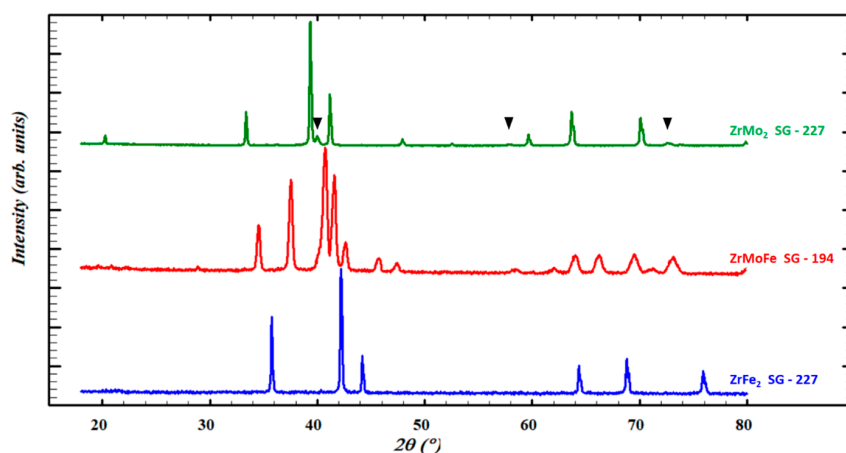


Figure 2. XRD patterns of $\text{Zr}(\text{Mo}_x\text{Fe}_{1-x})_2$, $x = 0, 0.5, 1$. Single-phased cubic C15 and hexagonal C14 Laves structures were found for ZrFe_2 (blue pattern) and ZrMoFe (red pattern), respectively. For ZrMo_2 , 95% C15 structure was found with 5% Mo (▼) (green pattern).

Table 1. Lattice constants, theoretical densities, porosities, longitudinal, v_L , and transverse, v_T , ultrasonic velocities, shear, G, and bulk, B, elastic moduli in the Laves phase $Zr(Mo_xFe_{1-x})_2$ system. Experimental B and G values of $Zr(Al_{0.04}Fe_{0.96})_2$ and theoretical B and G values of $ZrMo_2$ are also presented. The numbers in the parentheses present the estimated errors of the last significant digits.

x	a [Å]	c [Å]	Theoretical Density [kg/m ³]	Porosity [%]	v_L [m/s]	v_T [m/s]	G [GPa]	B [GPa]
0 *							75.8	148
[19]								
0	7.074		7614	0.9	5674 (9)	3142 (4)	75.6 (3)	148.2 (9)
0.5	5.173	8.461	8297	0.8	5337 (2)	2608 (1)	56.3 (2)	164.2 (4)
1	7.589		8605	0.7	5733 (16)	2762 (14)	66.1 (8)	200.4 (2)
1	7.594						57.3	196.5
[20]								

* $Zr(Al_{0.04}Fe_{0.96})_2$.

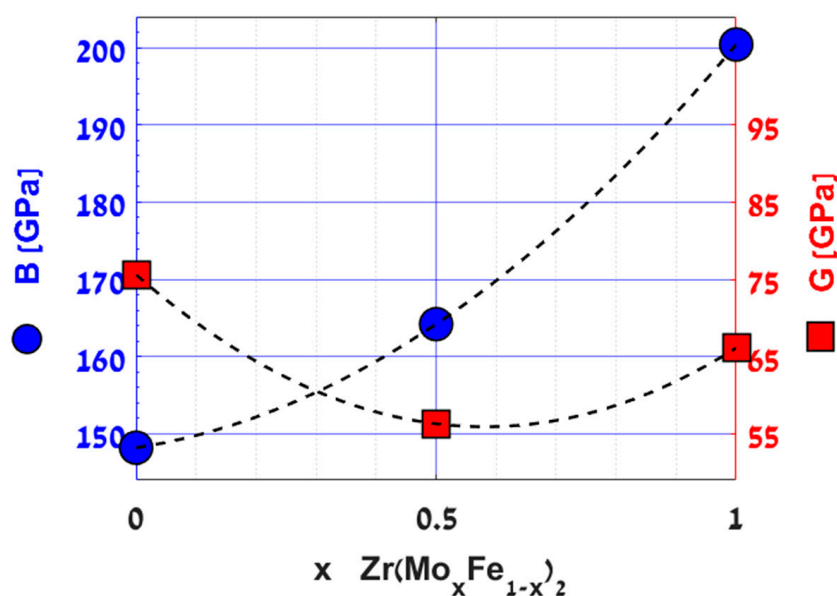


Figure 3. Bulk, B, and shear, G, moduli in $Zr(Mo_xFe_{1-x})_2$ intermetallic compounds.

$ZrMo_2$ absorbed about 2.1 H atoms per formula unit at 60 atm and room temperature, and about 3.5 H atoms per f.u. upon slow cooling to 78 K at 50 atm pressure. It should be born in mind that the hydrogenations of $ZrMo_2$ were carried out in order to estimate the corresponding v_H values. PCT (pressure-composition-temperature) isotherms of $ZrMo_2$ - H_2 may be found elsewhere, e.g., Ref. [11]. The XRD pattern, recorded immediately after removing the sample from the reactor, revealed two hydride phases, cubic Laves structure with lattice constant $a = 7.826 \text{ \AA}$ (26%) and tetragonal structure, space group 88, with cell parameters $a = 5.603 \text{ \AA}$, $c = 8.081 \text{ \AA}$ (68%) (Figure 4). These lattice constants slowly decreased during one week of exposure to the ambient atmosphere. The crystal parameter of Mo with dissolved Zr almost did not change ($a = 3.187 \text{ \AA}$) upon hydrogenation, indicating no hydrogen absorption in it. By imposing somewhat arbitrarily identical v_H for the two existing phases in $ZrMo_2H_{3.5}$, we obtain for the composition of these two phases $ZrMo_2H_{2.39}$ (MgCu₂-type, $a = 7.826 \text{ \AA}$) and $ZrMo_2H_{3.98}$ (tetragonal, SG88, $a = 5.603 \text{ \AA}$, $c = 8.081 \text{ \AA}$). Their common v_H is $2.2 \text{ \AA}^3/(\text{H atom})$. Additional v_H estimations, performed in a similar way for $ZrMo_2H_{1.6}$ and $ZrMo_2H_{2.8}$, yielded values between $2.1 \text{ \AA}^3/(\text{H atom})$ and $2.2 \text{ \AA}^3/(\text{H atom})$.

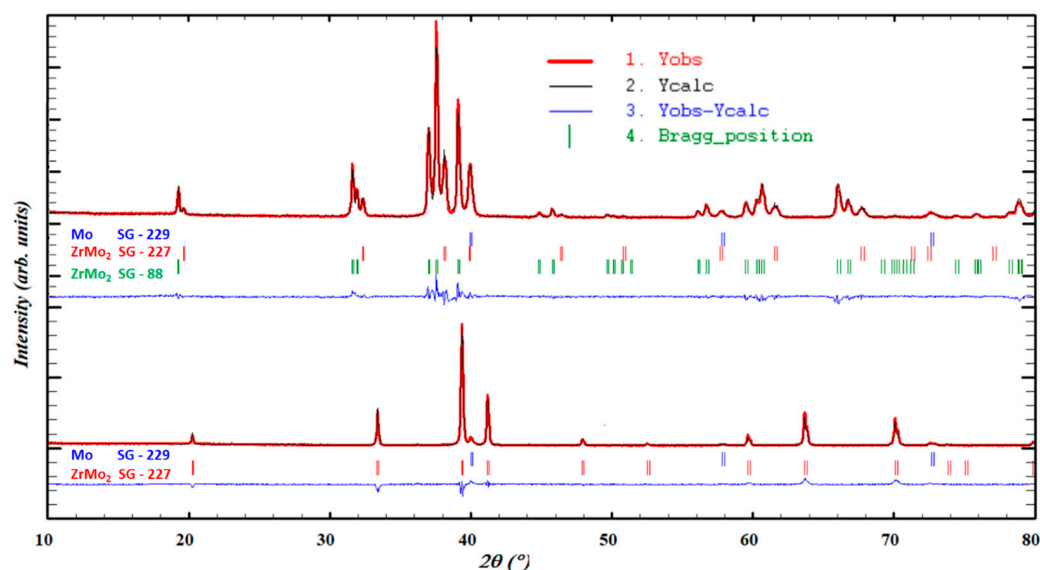


Figure 4. XRD pattern of $\text{ZrMo}_2\text{H}_{3.5}$ (upper plot) reveals the existence of two hydride phases (see also text). The pattern of ZrMo_2 before hydrogenation is shown in the lower plot for comparison.

3.2. Resolving the Peculiarity in the Stability Trends of the $\text{Zr}(\text{Mo}_x\text{Fe}_{1-x})_2$, $x = 0, 0.1, 0.5, 1$, Hydrides

As cited in the Introduction, the formation pressures of the $\text{Zr}(\text{Mo}_x\text{Fe}_{1-x})_2$ hydrides decrease between $x = 0$ and $x = 0.5$, indicating increasing stability in this compositional range. Then, this trend is unexpectedly reversed and ZrMo_2 hydride is formed at higher pressures than ZrMoFe and $\text{Zr}(\text{Mo}_{0.1}\text{Fe}_{0.9})_2$ hydrides. We consider next the possible factors influencing the stability of these hydrides.

3.2.1. The Substitution of Fe by Mo

Both Fe and Mo form hydrides at very high hydrogen pressures. The equilibrium formation pressure of $\text{MoH}_{1.1}$ and FeH are about 4.3 GPa at 600 °C and 3.5 GPa at 300 °C (decomposition pressure 2.2 GPa), respectively [21,22]. It is thus not expected that the hydrogen affinity properties of Mo, as compared to Fe, play a dominant role in the variation of the hydride stabilities in $\text{Zr}(\text{Mo}_x\text{Fe}_{1-x})_2$.

3.2.2. Trends of the Heats of Formation and the Crystal Volumes in the $\text{Zr}(\text{Mo}_x\text{Fe}_{1-x})_2$ System

Table 2 presents the crystal volumes per formula unit (f.u.), V , and theoretically derived heats of formation, ΔH_f , of the original, non-hydrogenated $\text{Zr}(\text{Mo}_x\text{Fe}_{1-x})_2$ intermetallics, $x = 0, 0.1, 0.5, 1$. The theoretically determined ΔH_f of 0.281 eV/(metal atom) for ZrFe_2 is in good agreement with a corresponding experimental value of 0.26 eV/(metal atom), e.g., Ref. [23]. ΔH_f values of $\text{Zr}(\text{Mo}_x\text{Fe}_{1-x})_2$, $x = 0.1, 0.5$ are obtained by interpolation.

Table 2. Unit cell volumes, V , heats of intermetallic formation, ΔH_f , hydrogen contents, hydrogen atomic volumes, v_H , and elastic interactions, u_{elas} , for $\text{Zr}(\text{Mo}_x\text{Fe}_{1-x})_2$ and the corresponding hydrides.

x	V [$\text{\AA}^3/\text{f.u.}$]	ΔH_f [eV/Atom]	H Content [H Atoms/f.u.]	v_H [$\text{\AA}^3/\text{H Atom}$]	u_{elas} [eV]
0 [24,25]	44.058	0.281 [26]	3.54	3.02	0.23
0.1 [25]	44.805	0.267	3.54	2.99	
0.5	48.089 [16]	0.21	2.5	2.90	0.17
	49.013 [15]		2.6	2.74	0.15
1	54.677 [27]	0.139 [28]	4	1.41	0.042
	54.829 [16]		1.4	1.57	0.052
	54.634 this work		3.5	2.2	0.102

The heats of formation of the intermetallic compounds decrease with x from 0.281 eV/(metal atom) for ZrFe_2 to 0.139 eV/(metal atom) for ZrMo_2 , while the corresponding crystal volumes increase from $44.058 \text{ \AA}^3/(\text{f.u.})$ to $54.634 \text{ \AA}^3/(\text{f.u.})$ (see Table 2). Thus, according to both the rule of reverse stability and the crystal volume criterion (see (i) and (ii) in the Introduction), the hydride stabilities should increase with x . These trends comply with the behavior for $0 \leq x \leq 0.5$, but disagree with the decreased stability of ZrMo_2 hydride.

3.2.3. Elastic Properties and H–H Elastic Interaction in $\text{Zr}(\text{Mo}_x\text{Fe}_{1-x})_2\text{-H}_2$

As already noted, the H–H interaction influences the critical temperature, T_c , according to Equation (1). It also contributes to the heat of hydrogen solution or hydride formation [6]. We find two indications for the reduction in the attractive, elastically mediated H–H interaction.

(a) From inspection of Figure 1, the very wide solubility region of $\text{ZrMo}_2\text{-H}_2$ indicates a decrease in T_c with respect to the rest of the hydrogenated $\text{Zr}(\text{Mo}_x\text{Fe}_{1-x})_2$ compounds, $x = 0, 0.1, 0.5$. This occurs in spite of the monotonic increase in the bulk modulus, B , from 148.2 GPa for ZrFe_2 to 200.4 GPa for ZrMo_2 , expected in turn to increase T_c .

(b) The increased hydrogenation pressures in $\text{ZrMo}_2\text{-H}_2$ with regard to $\text{Zr}(\text{Mo}_x\text{Fe}_{1-x})_2\text{-H}_2$, $x = 0.1, 0.5$, indicate a corresponding destabilization of ZrMo_2H_x . Indeed, the absolute enthalpy of ZrMo_2 hydride formation, 22 kJ/(mole H_2), is significantly lower than those of $\text{Zr}(\text{Mo}_x\text{Fe}_{1-x})_2$ hydrides, 29.5 kJ/(mole H_2) for $x = 0.5$, and 26 kJ/(mole H_2) for $x = 0.1$. It even approaches the 21.3 kJ/(mole H_2) for ZrFe_2 hydride [11]. This destabilization behavior suggests that the attractive (negative) contribution of the H–H elastic interaction to the enthalpy of hydride formation or to the enthalpy of hydrogen solubility in ZrMo_2 weakens with the increase in hydrogen content (see the similar case of $\text{TaV}_2\text{-H}_2$ below).

As the variation in B of the $\text{Zr}(\text{Mo}_x\text{Fe}_{1-x})_2$ compounds cannot directly account for the observed trend in the critical temperatures of the metal-to-hydride phase transitions and the heats of hydride formation at $x > 0.5$, we inspect another term that appears in a squared form in Equation (2), namely, v_H . A priori, v_H is not supposed to significantly affect u_{elas} according to Equation (2), as v_H usually acquires values in quite a narrow range, e.g., Ref. [6]. We find hereafter surprising experimentally derived v_H values. Lushnikov et al. report that a Laves ZrMo_2 compound with lattice constant $a = 7.591 \text{ \AA}$ undergoes a tetragonal distortion upon deuteration to ZrMo_2D_4 with lattice constants $a = 5.496 \text{ \AA}$ and $c = 7.986 \text{ \AA}$ [27]. The authors note that such a tetragonal distortion is a known phenomenon in hydrogenated Laves phase compounds [29]. It is also worth noting that the composition of the interstitial sites does not change upon the tetragonal distortion. The deuterium atoms occupy ($2\text{Zr} + 2\text{Mo}$) tetrahedral interstitial sites [27], which are the preferable ($2A + 2B$) sites for hydrogen occupation in AB_2 Laves phase compounds [30]. A straightforward evaluation of the volume of the hydrogen atom in ZrMo_2D_4 (4 f.u./unit cell), using also the above data for ZrMo_2 (8 f.u./unit cell), yields $v_H = 1.4 \text{ \AA}^3/(\text{H atom})$. This is the lowest reported v_H value in intermetallic and even in binary hydrides [6] (pp. 105–109). Supporting evidence for this hydrogen atomic volume may be found in the reported cell parameter $a = 7.698 \text{ \AA}$ of $\text{ZrMo}_2\text{H}_{1.4}$ [16]. Utilizing $a = 7.598 \text{ \AA}$ for ZrMo_2 by the same authors [31], $v_H = 1.6 \text{ \AA}^3/(\text{H atom})$ is evaluated. It should be noted that a cell parameter $a = 7.548 \text{ \AA}$ is reported for ZrMo_2 in [16], which is very different from other reported values [13,27], as well as from the value, reported later, by the same authors [31]. Nonetheless, v_H of $2.33 \text{ \AA}^3/(\text{H atom})$ is obtained for $\text{ZrMo}_2\text{H}_{1.4}$ by employing $a = 7.548 \text{ \AA}$ for ZrMo_2 , although the stated v_H in [16] is $2.6 \text{ \AA}^3/(\text{H atom})$. Additional v_H values, reported for various hydrogen compositions in ZrMo_2 , span between 3.2 and $4.5 \text{ \AA}^3/(\text{H atom})$ [31]. We recommend adopting $v_H = 2.2 \text{ \AA}^3/(\text{H atom})$ for the ZrMo_2 hydrides following the experimental estimations of this work. It is worthwhile noting that we found larger lattice constants of the tetragonal hydride phase (see Section 3.1) than those cited above. The latter lattice constants were obtained in the course of a seemingly very comprehensive neutron diffraction experiment, under much more extreme conditions of 2500 atm hydrogen pressure and a temperature of 78 K [27]. Table 2 presents the relevant information for the $\text{Zr}(\text{Mo}_x\text{Fe}_{1-x})_2$ compounds and their hydrides. The small values of v_H affect u_{elas} very significantly. Table 2 lists

the calculated values of u_{elas} according to Equation (2), utilizing the measured bulk and shear moduli (Table 1), and the V and v_{H} volumes (Table 2). The $\text{ZrMo}_2\text{-H}_2$ system clearly exhibits the smallest v_{H} and u_{elas} . This may explain the decreased T_{c} in this system according to Equation (1). The hydride stability would also be decreased as u_{elas} provides a smaller negative contribution to the heat of hydride formation of ZrMo_2 with regard to ZrFe_2 and ZrMoFe . A most probable reason for the decrease in v_{H} , and hence in u_{elas} , in the $\text{Zr}(\text{Mo}_x\text{Fe}_{1-x})_2$ system is the large bulk modulus of ZrMo_2 . We suggest that the large bulk modulus of ZrMo_2 confines the expansion of the metal lattice upon hydrogenation by restricting the H atoms in smaller interstitial volumes, v_{H} . The variation of v_{H} as a function of B , plotted in Figure 5, supports this suggestion. The depressed expansion of the crystal lattice mitigates the strain fields around a hydrogen atom and thus reduces the elastically mediated interaction between the hydrogen atoms.

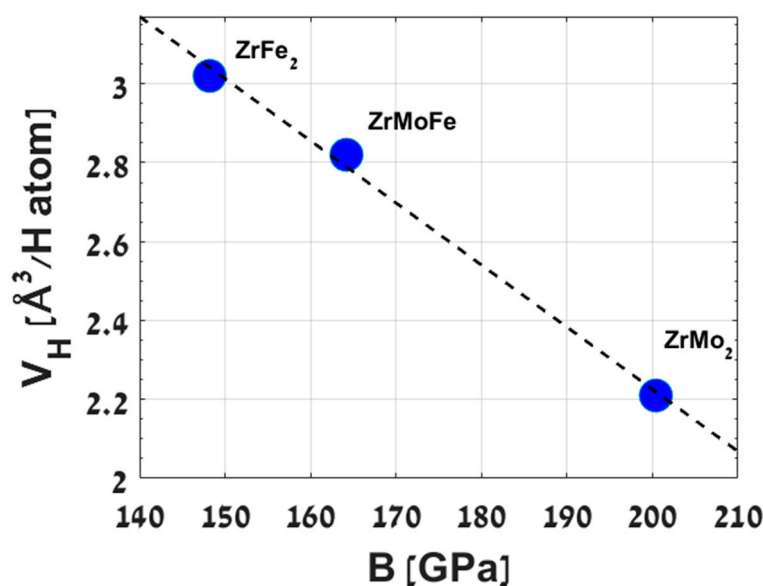


Figure 5. Variation of the hydrogen atomic volume, v_{H} , in the hydrogenated $\text{Zr}(\text{Mo}_x\text{Fe}_{1-x})_2$, $x = 0, 0.5, 1$, compounds as a function of the bulk moduli, B , of the corresponding original intermetallics.

Elastic moduli rarely play such a significant role in the hydrogenation properties of intermetallic compounds. We note that a very similar behavior to that of $\text{ZrMo}_2\text{-H}_2$ is demonstrated by the C15 compound TaV_2 . The experimentally derived bulk modulus of C15 TaV_2 varies between 200 GPa at low temperatures and 194 GPa at room temperature [32]. These B values of TaV_2 are very close to the 200.4 GPa bulk modulus of ZrMo_2 , obtained in this work (see Table 1 and Figure 5). The volume of the hydrogen atom in hydrogenated TaV_2 is $2.09 \text{ \AA}^3/(\text{H atom})$ [33] in the low range of v_{H} values, and in close proximity to v_{H} of $2.2 \text{ \AA}^3/(\text{H atom})$, estimated here for the hydrogenated ZrMo_2 (see Table 2 and Figure 5). Accordingly, $\text{TaV}_2\text{-H}_2$ exhibits a broad solid hydrogen solubility region without a discontinuous metal-to-hydride phase transition even at temperatures as low as 195 K and pressures of 1000 atm [33]. In addition, the heat of hydrogen solution decreases with the increase in H content, i.e., becomes less exothermic. This may be regarded as surmounting the attractive elastic H–H interaction by some repulsive, probably electronic H–H interaction. It is worthwhile noting that the heats of hydrogen solution in metal–hydrogen systems usually become more exothermic with the increase in H content, e.g., Refs. [6,34]. We suggest that, in resemblance to $\text{ZrMo}_2\text{-H}_2$, the large bulk modulus of TaV_2 confines the hydrogen atoms into small interstitial volumes and consequently reduces the H–H elastic interaction, as indicated by the broad solubility region and the lack of metal to hydride phase transition in $\text{TaV}_2\text{-H}_2$. Another example of a significant role of elastic moduli is the shear stiffening in $\text{Zr}(\text{Al}_x\text{M}_{1-x})_2$, $\text{M}=\text{Fe}, \text{Co}$ [19,35]. It prevents hydrogen absorption in ZrAl_2 even at extremely high H_2 pressures of 40 GPa [36], although

Al substitution drastically stabilizes the hydrogen absorption of $ZrFe_2$ and $ZrCo_2$ for small x values [37,38].

4. Summary and Conclusions

The elastic moduli of $Zr(Mo_xFe_{1-x})_2$, $x = 0, 0.5, 1$, as well as hydrogen absorption in $ZrMo_2$, were measured in an attempt to shed light on the unusual trend of hydride stabilities in this system. It seems that the bulk modulus plays a dual role in that context. Initially, B participates in generating attractive elastic interaction between the hydrogen atoms. Then, the significant increase in B in $ZrMo_2$ confines the expansion of the metal matrix and restrains the hydrogen atoms in smaller interstitial volumes. Consequently, the attractive H–H interaction is reduced, demonstrated by a sharp decrease in the critical temperature for metal-to-hydride phase transition and the hydride stability in the $ZrMo_2$ - H_2 system. We also suggest a similar explanation for the lack of a discontinuous metal-to-hydride phase transition in the Laves phase TaV_2 - H_2 system. It would be of interest to find a criterion that determines at which point B converts from a stabilizing to destabilizing agent during hydrogen absorption in intermetallic systems.

Author Contributions: Conceptualization, I.J.; methodology, D.B. and M.B.; validation, D.B. and M.B.; formal analysis, D.B.; investigation, D.B. and M.B.; writing—original draft preparation, I.J.; writing—review and editing, D.B., R.Z.S. and I.J.; supervision, I.J. and R.Z.S.; funding acquisition, I.J. and R.Z.S. All authors have read and agreed to the published version of the manuscript.

Funding: This research was partly funded by the Israel Science Foundation grant number 745/15.

Acknowledgments: This research was partly supported by the Israel Science Foundation (grant No. 745/15). One of the authors (IJ) is grateful to S. Mitrokhin for granting access to his presentation at MH2018, as well as for turning attention to the unusual stability trends of the $Zr(Mo_xFe_{1-x})_2$ hydrides.

Conflicts of Interest: The authors declare no conflict of interest.

References

1. Reilly, J.J. Chemistry of intermetallic hydrides, BNL report 46778, presented at the Symposium for Hydrogen Storage Materials, Battery and Electrochemistry. In Proceedings of the 180th Meeting of the Electrochemical Society, Phoenix, AZ, USA, 13–18 October 1991.
2. van Mal, H.H.; Buschow, K.H.J.; Miedema, A.R. Hydrogen absorption in $LaNi_5$ and related compounds: Experimental observations and their explanation. *J. Less-Common Met.* **1974**, *35*, 65–76. [CrossRef]
3. Lartigue, C. Etude Structurale et Thermodynamique du Systeme $LaNi_{5-x}Mn_x$ —Hydrogene. Ph.D. Thesis, Universite Paris VI, Paris, France, 1984.
4. Jacob, I.; Hadari, Z.; Reilly, J.J. Hydrogen absorption in $ANiAl$ ($A = Zr, Y, U$). *J. Less-Common Met.* **1984**, *103*, 123–127. [CrossRef]
5. Biderman, S.; Jacob, I.; Mintz, M.H.; Hadari, Z. Analysis of the hydrogen absorption in the $U(Al_xNi_{1-x})_2$ system. *Trans. Nucl. Soc. Isr.* **1982**, *10*, 129–132.
6. Fukai, Y. *The Metal-Hydrogen System: Basic Bulk Properties*, 2nd ed.; Springer: Berlin/Heidelberg, Germany, 2005.
7. Alefeld, G. Phase transitions of hydrogen in metals due to elastic interaction. *Ber. Bunsenges. Phys. Chem.* **1972**, *76*, 746–755.
8. Wagner, H. Elastic Interaction and phase transition in coherent metal-hydrogen systems. In *Hydrogen in Metals I*; Alefeld, G., Völkl, J., Eds.; Springer: Berlin/Heidelberg, Germany, 1978; pp. 5–51.
9. Li, F.; Zhao, J.; Tian, D.; Zhang, H.; Ke, X.; Johansson, B. Hydrogen storage behavior in C15 Laves compound $TiCr_2$ by first principles. *J. Appl. Phys.* **2009**, *105*, 043707. [CrossRef]
10. Babai, D.; Bereznitsky, M.; Shneck, R.Z.; Jacob, I. The effect of Pd on hydride formation in $Zr(Pd_xM_{1-x})_2$ intermetallics where M is a 3d element. *J. Alloys Compd.* **2021**, *889*, 161503. [CrossRef]
11. Mitrokhin, S.; Verbetsky, V. Peculiarities of Hydrogen Interaction with Alloys of $ZrFe_2$ - $ZrMo_2$ System. *Int. J. Hydrogen Energy* **2019**, *44*, 29166–29169. [CrossRef]
12. Muraoka, Y.; Shiga, M.; Nakamura, Y. Magnetic properties and Mössbauer effect of $A(Fe_{1-x}B_x)_2$ ($A = Y$ or Zr , $B = Al$ or Ni) Laves phase intermetallic compounds. *Phys. Status Solidi* **1977**, *42*, 369–374. [CrossRef]
13. Domagala, R.F.; McPherson, D.J.; Hansen, M. Systems Zirconium-Molybdenum and Zirconium-Wolfram. *JOM* **1953**, *5*, 73–79. [CrossRef]
14. Straumanis, M.E.; Shodhan, R.P. Lattice Constants, Thermal Expansion Coefficients and Densities of Molybdenum and the Solubility of Sulphur, Selenium and Tellurium in it at 1100 °C. *Z. Metallkd.* **1968**, *59*, 492–495. [CrossRef]
15. Yartys, V.A.; Burnasheva, V.V.; Fadeeva, N.V.; Solov'ev, S.P.; Semenenko, K.N. The crystal structure of the deuteride $ZrMoFeD_{2.6}$. *Sov. Phys. Crystallogr. (Transl. Krist.)* **1982**, *27*, 540–543.

16. Semenenko, K.N.; Verbetskii, V.N.; Mitrokhin, S.V.; Burnasheva, V.V. Investigation of the interaction with hydrogen of Zirconium intermetallic compounds crystallised in Laves phase structure types. *Russ. J. Inorg. Chem.* **1980**, *25*, 961–964, Translated from *Zhurnal Neorgamicheskoi Khimii* **1980**, *25*, 1731–1736.
17. Mackenzie, J.K. The elastic constants of a solid containing spherical holes. *Proc. Phys. Soc. B* **1950**, *63*, 2–11. [[CrossRef](#)]
18. Masi, L.; Borch, E.; de Gennaro, S. Porosity behavior of ultrasonic velocities in polycrystalline Y-B-C-O. *J. Phys. D Appl. Phys.* **1996**, *29*, 2015–2019. [[CrossRef](#)]
19. Willis, F.; Leisure, R.G.; Jacob, I. Elastic moduli of the Laves-phase pseudobinary compounds $Zr(Al_xFe_{1-x})_2$ as determined by ultrasonic measurements. *Phys. Rev. B* **1994**, *50*, 13792–13794. [[CrossRef](#)]
20. Turkdal, N.; Deligoz, E.; Ozisik, H.; Ozisik, H.B. First-principles studies of the structural, elastic, and lattice dynamical properties of $ZrMo_2$ and $HfMo_2$. *Phase Transit.* **2017**, *90*, 598–609. [[CrossRef](#)]
21. Abramov, S.N.; Antonov, V.E.; Bulychev, B.M.; Fedotov, V.K.; Kulakov, V.I.; Matveev, D.V.; Sholin, I.A.; Tkacz, M. T-P phase diagrams of the Mo-H system revisited. *J. Alloys Compd.* **2016**, *672*, 623–629. [[CrossRef](#)]
22. Tkacz, M. Thermodynamic properties of iron hydride. *J. Alloys Compd.* **2002**, 330–332, 25–28. [[CrossRef](#)]
23. Klein, R.; Jacob, I.; O'Hare, P.A.G.; Goldberg, R.N. Solution-calorimetric determination of the standard molar enthalpies of formation of the pseudobinary compounds $Zr(Al_xFe_{1-x})_2$ at the temperature 298.15 K. *J. Chem. Thermodyn.* **1994**, *26*, 599–608. [[CrossRef](#)]
24. Zotov, T.; Movlaev, E.; Mitrokhin, S.; Verbetsky, V. Interaction in $(Ti,Sc)Fe_2-H_2$ (Zr,Sc) Fe_2-H_2 systems. *J. Alloys Compd.* **2008**, 459, 220–224. [[CrossRef](#)]
25. Zotov, T.A.; Sivov, R.B.; Movlaev, E.A.; Mitrokhin, S.V.; Verbetsky, V.N. IMC hydrides with high hydrogen dissociation pressure. *J. Alloys Compd.* **2011**, *509*, S839–S843. [[CrossRef](#)]
26. The Materials Project. Available online: <https://materialsproject.org/materials/mp-1718/> (accessed on 9 April 2023).
27. Lushnikov, S.A.; Movlaev, E.A.; Verbetsky, V.N.; Somenlov, V.A.; Agafonov, S.S. Interaction of $ZrMo_2$ with hydrogen at high pressure. *Int. J. Hydrogen Energy* **2017**, *42*, 29166–29169. [[CrossRef](#)]
28. The Materials Project. Available online: <https://materialsproject.org/materials/mp-2049/> (accessed on 9 April 2023).
29. Irodova, A.V.; Glazkov, V.P.; Somenkov, V.A.; Shilstein, S.S. Hydrogen ordering in the cubic Laves phase HfV_2 . *J. Less-Common Met.* **1981**, *77*, 89–98. [[CrossRef](#)]
30. Jacob, I.; Bloch, J.M.; Shaltiel, D.; Davidov, D. On the occupation of interstitial sites by hydrogen atoms in intermetallic hydrides: A quantitative model. *Solid State Commun.* **1980**, *35*, 155. [[CrossRef](#)]
31. Semenenko, K.N.; Verbetskii, V.N.; Pilchenko, V.A. Interaction of $ZrMo_2$ with hydrogen at low temperatures. *Mosc. Univ. Chem. Bull. (Transl. Vestn. Mosk. Univ. Ser. 2)* **1986**, *41*, 131–133.
32. Foster, K.; Hightower, J.E.; Leisure, R.G.; Skripov, A.V. Elastic moduli of the C15 Laves-phase materials TaV_2 , $TaV_2H(D)_x$ and $ZrCr_2$. *Philos. Mag. B* **2000**, *80*, 1667–1679. [[CrossRef](#)]
33. Lynch, J.F. The solution of hydrogen in TaV_2 . *J. Phys. Chem. Solids* **1981**, *42*, 411–419. [[CrossRef](#)]
34. Bereznitsky, M.; Mogilyanski, D.; Jacob, I. Destabilizing effect of Al substitution on hydrogen absorption in $Zr(Al_xV_{1-x})_2$. *J. Alloys Compd.* **2012**, *542*, 213–217. [[CrossRef](#)]
35. Jacob, I.; Bereznitsky, M.; Yeheskel, O.; Leisure, R.G. Role of shear stiffening in reducing hydrogenation in intermetallic compounds. *Appl. Phys. Lett.* **2006**, *89*, 201909. [[CrossRef](#)]
36. Machida, A. Unpublished Results.
37. Bereznitsky, M.; Jacob, I.; Bloch, J.; Mintz, M.H. Thermodynamic and structural aspects of hydrogen absorption in the $Zr(Al_xCo_{1-x})_2$ system. *J. Alloys Compd.* **2002**, *346*, 217. [[CrossRef](#)]
38. Bereznitsky, M.; Jacob, I.; Bloch, J.; Mintz, M.H. Thermodynamic and structural aspects of hydrogen absorption in the $Zr(Al_xFe_{1-x})_2$ system. *J. Alloys Compd.* **2003**, *351*, 180. [[CrossRef](#)]

Disclaimer/Publisher's Note: The statements, opinions and data contained in all publications are solely those of the individual author(s) and contributor(s) and not of MDPI and/or the editor(s). MDPI and/or the editor(s) disclaim responsibility for any injury to people or property resulting from any ideas, methods, instructions or products referred to in the content.